JOURNAL OF MATERIALS SCIENCE 27 (1992) 1869–1875

Oxidation of TiC at low temperatures

S. SHIMADA, M. KOZEKI*
Department of Applied Chemistry, Faculty of Engineering, Hokkaido University, West 8, North 13, Kitaku, Sapporo 060, Japan

The isothermal oxidation of TiC powders was carried out at low temperatures of 350–500 °C at oxygen pressures of 3.9, 7.9 and 16 kPa under a static total pressure of 39.5 kPa, achieved by mixing with argon, using an electro-microbalance. The oxidation kinetics are described by the one-dimensional diffusion equation. It was found that oxidation consists of four steps, I (fast step), II (slow step), III (fast step) and IV (slow step), at all the pressures. Two activation energies were obtained in steps II–IV: 125–150 kJ mol^{-1} below about 420 °C and 42–71 kJ mol^{-1} above that temperature. The low- and high-temperature oxidation mechanisms are discussed in connection with the formation of oxycarbide/titanium suboxides and the crystallization of anatase, followed by the generation of cracks in the grains.

1. Introduction

Titanium carbide (TiC) has interesting possibilities as engineering materials because of its extremely high melting point and strength, and good corrosion resistance [1]. Although TiC has such attractive properties, poor oxidation resistance at high temperatures tends to restrict its range of applications.

Several oxidation studies on TiC materials have been reported [2–7]. Of these, Reichle and Nickl [3] have studied the oxidation of pure single crystals with the composition of $TiC_{1.00}$ in oxygen, oxygen/argon mixture, carbon dioxide and carbon dioxide/carbon monoxide mixture at temperatures of 800–1200 °C. They have observed the parabolic kinetics at oxygen partial pressures (P_{O_2}) of 1.3–39.5 kPa, the transition from parabolic to linear rates above 39.5 kPa and the linear kinetics below 13 Pa. Lavrenko *et al.* [4] carried out the oxidation of hot-pressed TiC materials at P_{O_2} = 13 Pa–100 kPa and temperatures of 700–1200 °C, and reported that the oxidation process follows the parabolic law within the first 40–50 min, after which oxidation proceeds paralinearly. Stewart *et al.* [5] studied the effect of temperature (400–850 °C) and oxygen partial pressure (1.2–85 kPa) on the oxidation of TiC powders, and found that the parabolic oxidation proceeds with an activation energy of 192 kJ mol^{-1} above 600 °C. Haglund *et al.* [6] performed the oxidation of TiC-coated cemented carbide under a normal atmosphere at 600–1000 °C, and reported that the oxidation rate changes from a parabolic law at 600–700 °C, to a linear law above 900 °C.

These studies have revealed that the oxidation of TiC parabolically proceeds at intermediate pressures (several to 100 kPa) and at temperatures of 600–800 °C, in contrast to the linear oxidation at higher pressures and temperatures. The studies have also reported that the oxidized product forms the double layers consisting of TiO_2 (rutile) (in the outer layer) and oxycarbide or titanium suboxide (in the inner layer) [4, 6, 7].

On the other hand, there have been few works on the low-temperature oxidation of TiC below 600 °C, and nor has it been elucidated how the formation of anatase contributes to the oxidation of TiC. A previous paper described the oxidation kinetics of ZrC at relatively low temperatures and established the oxidation mechanism, as well as, for the first time, the formation of diamond [8]. This study, as a continuation of the experimental programme of oxidation of transition metal carbides, reports the oxidation of TiC at low temperatures of 350–500 °C at oxygen pressures of 3.9, 7.9 and 16 kPa, to provide further information about the oxidation mechanism involved.

2. Experimental procedure

The starting material was commercial titanium carbide (purity 99.5%). The major impurities contained in TiC powders were, as reported by the supplier, Si < 0.03%, Fe < 0.03%, Mg < 0.001%, Cu < 0.001%, Nb < 0.1%. The lattice parameter of TiC powders was determined to be $a_0 = 0.4327 \pm 0.0001$ nm, from which the atomic ratio of C/Ti in the TiC was estimated to be 0.97, according to the relationship between the ratio C/Ti and the lattice parameter [1]. The grains of TiC were of angular platy shape as observed by scanning electron microscopy (SEM). The surface area of the TiC sample was 9.9 m^2 g^{-1}, as measured by the BET method. The grain sizes were measured by the centrifugal sedimentation method and had a mean diameter of about 2 μm.

* *Present address*: Cannon Co. Ltd, Tokyo, Japan.

0022–2461

The weight changes of the TiC sample (40 mg) during oxidation were monitored at a fixed temperature of 350–500 °C using an electro-microbalance. The isothermal oxidation was performed under a total partial pressure of 39.5 kPa. The oxygen partial pressures, achieved by mixing with argon, were 3.9, 7.9 and 16 kPa. The detailed experimental procedure was reported previously [8].

The phases present in the sample after oxidation were identified by X-ray powder diffraction (XRD), and the morphology of the oxidized TiC grains was observed by SEM. Electron microdiffraction (EMD) on the edges of the oxidized TiC grains was carried out under an accelerating voltage of 200 kV. A simultaneous thermogravimetry–differential thermal analysis (TG–DTA) experiment for oxidation of TiC powders was carried out at a heating rate of 5 °C min^{-1} under atmospheric pressure.

3. Results

The fraction reacted, α, during oxidation was calculated by dividing the measured weight increase by the theoretical one, calculated by assuming the complete conversion of TiC to TiO_2 according to the equation

$$TiC_{0.97} + 1.97\,O_2 = TiO_2 + 0.97\,CO_2 \quad (1)$$

The isothermal oxidation was carried out under oxygen pressures of 3.9, 7.9 and 16 kPa at temperatures of 350–500 °C. The measured fractions were reproducible within $\pm$ 4%. As a result of applying to various rate equations, the oxidation rates were found to be best described up to around 70% by the one-dimensional diffusion-controlling equation

$$\alpha^2 = kt \quad (2)$$

where k is the rate constant and t the time.

Figs 1–3 show the plots of α^2 versus t on oxidation at P_{O_2} = 3.9, 7.9 and 16 kPa, respectively. The kinetic plots give a broken line inflected at fixed fractions at each temperature and pressure. It was found that oxidation essentially consists of four steps, designated I, II, III and IV, as exemplified from the plots at 7.9 kPa: step I (fast step) covers a range below 10%, step II (slow step) a range between 10% and 18% –33%, step III (fast step) a range between 18%–33% and 45%, and step IV (slow step) a range above 45%. The fraction range covering each step varies, depending on the temperature and pressure.

At 3.9 kPa (Fig. 1), the initial straight lines go almost through the origin. At temperatures of 350–400 °C, the oxidation rates are the same as in steps I and II, increasing at a fraction of ~ 30% near the onset of step III. Oxidation in step III goes up to 60% without giving rise to step IV. Above 424 °C, oxidation in steps I–III proceeds apparently in one step up to about 50%, slowing down in step IV.

At 7.9 kPa (Fig. 2), the initial straight lines do not go through the origin, but intersect the ordinate corresponding to a fraction of 10%. This indicates that oxidation occurs rapidly within a few minutes in step I. As the temperature increases from 352 °C to 452 °C, a boundary point between steps II and III decreases from 33% to 18%, finally disappearing at 500 °C. A

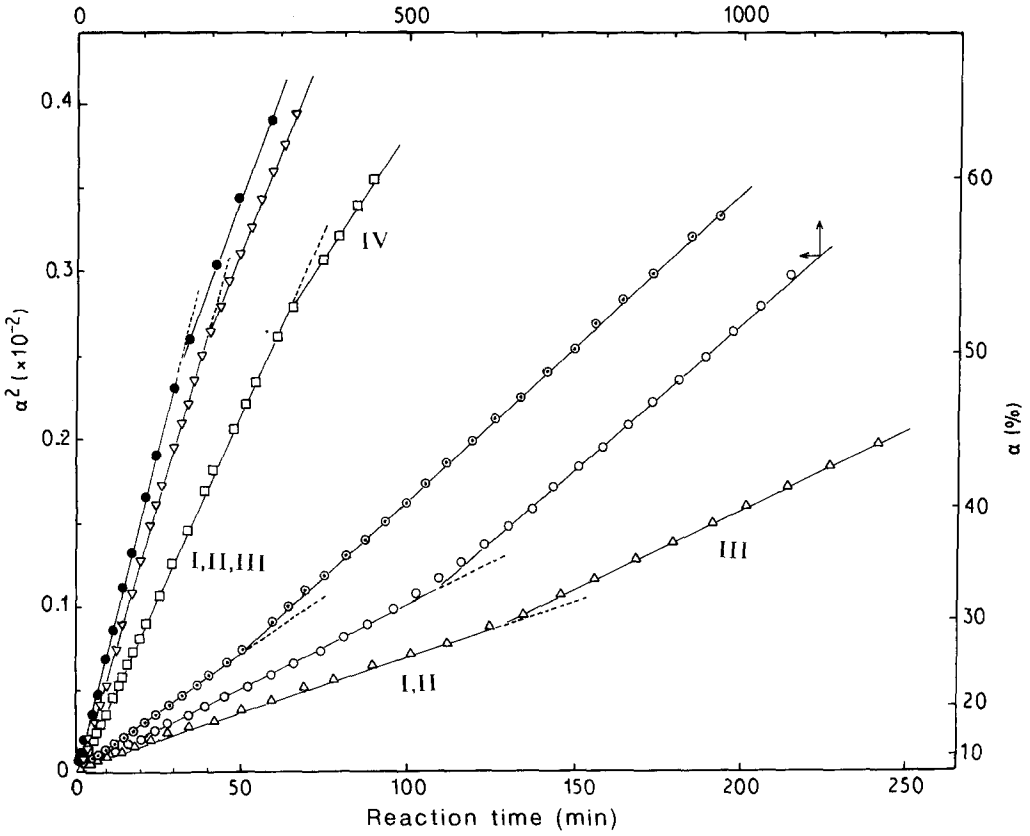

Figure 1 Plots of α^2 versus t for the isothermal oxidation kinetics of TiC at 3.9 kPa. Reaction temperature (°C): (○) 350, (△) 378, (⊙) 400, (□) 424, (▽) 454, (●) 500.

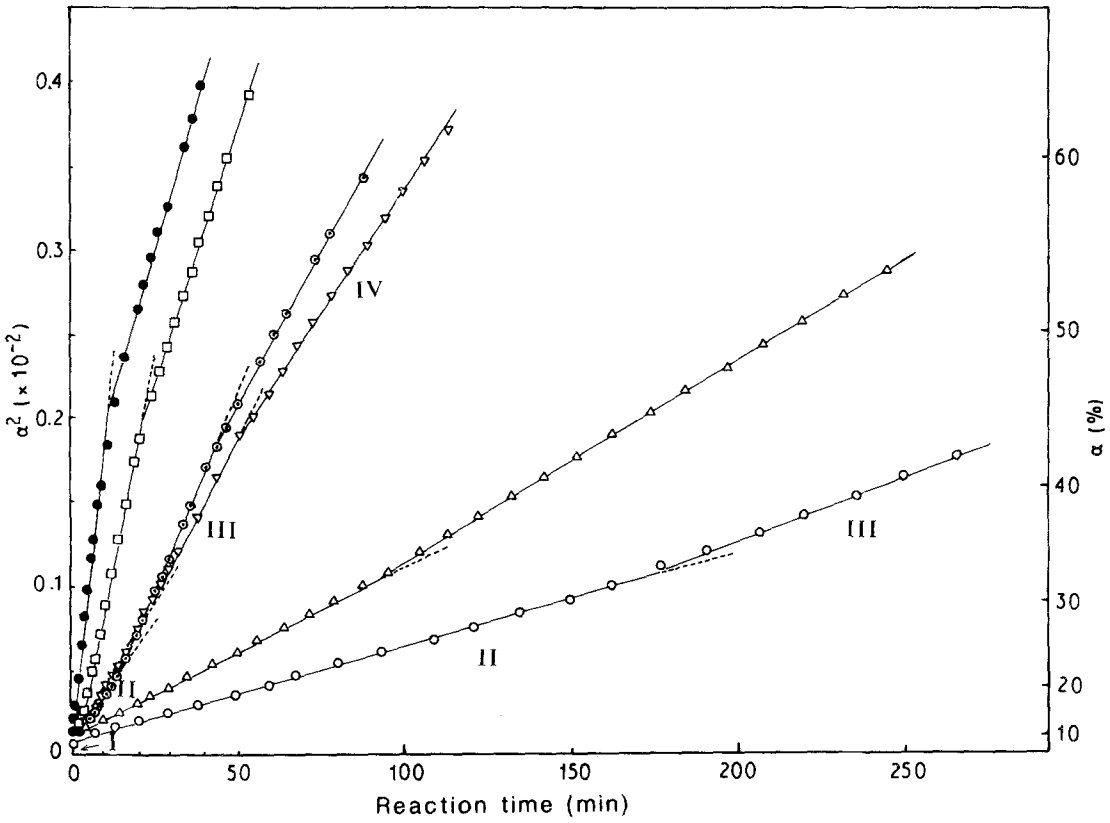

Figure 2 Plots of α^2 against t for the isothermal oxidation kinetics of TiC at 7.9 kPa. Reaction temperature (°C): (○) 352, (△) 379, (▽) 400, (⊙) 426, (□) 452, (●) 500.

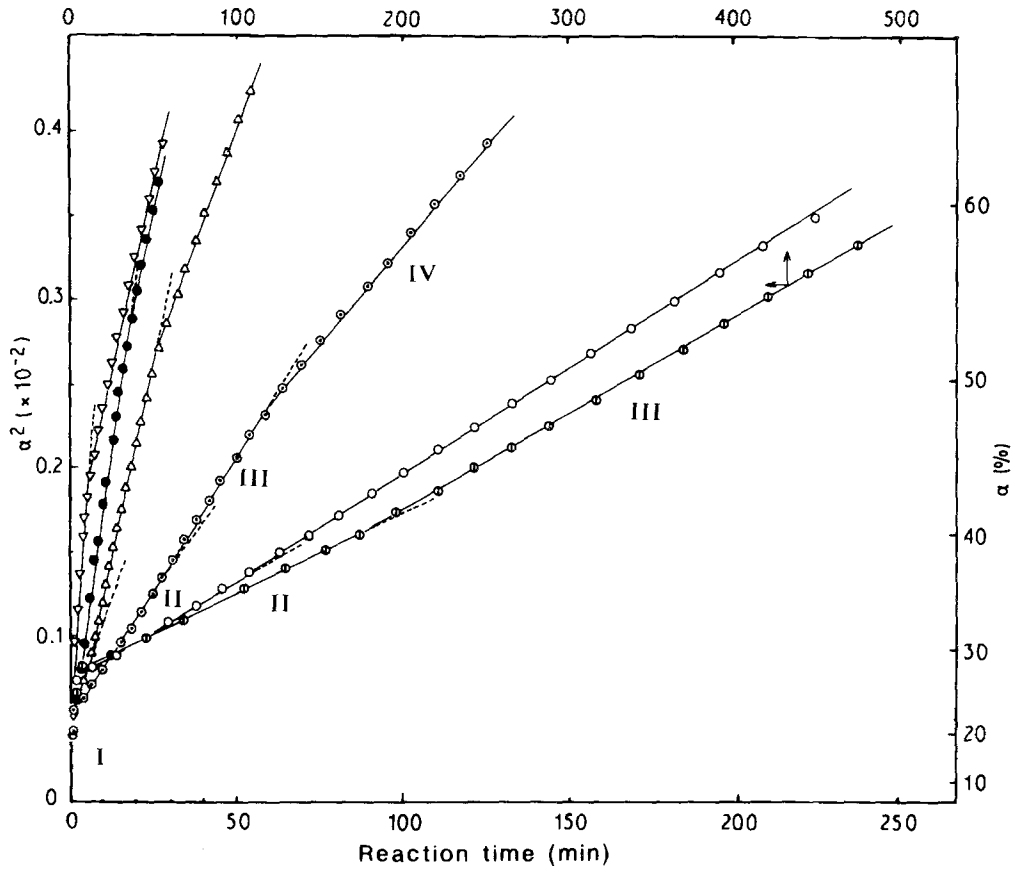

Figure 3 Plots of α^2 against t for the isothermal oxidation kinetics of TiC at 16 kPa. Reaction temperature (°C): (Φ) 355, (○) 376, (⊙) 400, (△) 426, (●) 445, (▽) 500.

transition from step III to IV is not observed at 352 and 379 °C, but occurs around 45% at 403–500 °C. At 500 °C, oxidation proceeds apparently in two steps.

At 16 kPa (Fig. 3), the early straight lines intersect the ordinate corresponding to the fraction of about 20%, suggesting rapid oxidation in step I. The starting fraction of steps II–IV is about 10% higher than that at 3.9 and 7.9 kPa. At temperatures of 355 and 376 °C, a transition from step II to III occurs around 40%, but step IV is not observed. Four steps, I–IV appear at 400 and 426 °C. Above 445 °C, steps II and III occur concurrently.

The Arrhenius plots of ln k versus $1/T$ at 3.9, 7.9 and 16 kPa are shown in Fig. 4, in which the k values in steps II–IV were obtained from the slopes in Figs 1–3. The plots change their slopes at the temperature of 410–450 °C. The low-temperature region has an activation energy of 125–150 kJ mol^{-1}, the high-temperature region has one of 42–71 kJ mol^{-1}.

Figs 5 and 6 show X-ray diffraction patterns of the samples oxidized to various fractions at 3.9 and 7.9 kPa, respectively, at 400 °C. At 3.9 kPa (Fig. 5a–d), no peaks corresponding to TiO_2 are seen at 17%, but a small broad peak of TiO_2 (anatase) appears at 27%, increasing with increasing fraction (b to d). A very slight formation of rutile-type TiO_2 is noticed around 66% in step IV (c). The amount of rutile formed is still small at 95% (d). At 7.9 kPa (Fig. 6a–f), the formation of TiO_2 is not seen at 13% on initial rapid oxidation (a). A broad peak of anatase appears at a fraction of 27%, which is near the end of step II, then increasing with increasing fraction (b–f). A very slight formation of rutile can be seen at 52%–58% in step IV (d and e). The amount of anatase formed is greater than that of rutile at 94% (f). Even at this fraction, the diffraction lines of TiC are still observed. At 16 kPa and 400 °C, rutile, in addition to anatase, was found to be already formed at 25% on initial rapid oxidation, and the amount of rutile formed was comparable to that of anatase in steps II–IV.

The EMD results at 3.9 and 16 kPa indicated that the titanium suboxides, TiO (d_{obs} = 0.210, 0.200, 0.145 nm), Ti_3O_5 (d_{obs} = 0.270, 0.184, 0.154 nm) and Ti_4O_7 (d_{obs} = 0.305, 0.286 nm) [9], are formed on edges of the grains of the samples obtained at the 6% fraction and that the Ti_2O_3 phase (d_{obs} = 0.372, 0.178, 0.156 nm) [9] in addition to anatase, is present in the samples oxidized to 40%.

The plots of log (rate constant, k) versus log (oxygen pressure, P_{O_2}) are shown in Fig. 7, to explain the effect of oxygen pressure on the oxidation rate. Their relations are expressed by an equation, $\log k = n \log P_{O_2}$ with n = 0.2–0.6 at temperatures of 350 and 376 °C. Above 400 °C, the rates at 7.9 kPa are similar to or greater than those at 16 kPa.

The effect of oxygen pressure on the formation of anatase and rutile at low temperatures is shown in Fig. 8, which presents X-ray diffraction patterns of the samples oxidized to the fractions of 89%–92% at 350 °C. The formation of anatase is seen at the three pressures. Rutile is not or is only very slightly formed at 3.9 or 7.9 kPa, respectively, but is considerably formed at 16 kPa. It was shown in Figs 5 and 6 that a

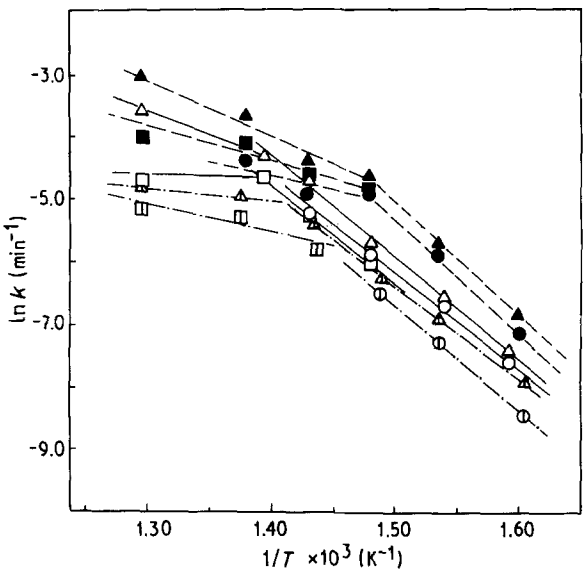

Figure 4 Arrhenius plots of rate constants versus reciprocal temperature. (—·—·—, ⧋, ▥) 3.9 kPa, (——, ○, □) 7.9 kPa, (— — —, ▲, ■, ●) 16 kPa (○, ●) Stage II, (△, ▲, ⧋) stage III, (□, ■, ▥) stage IV.

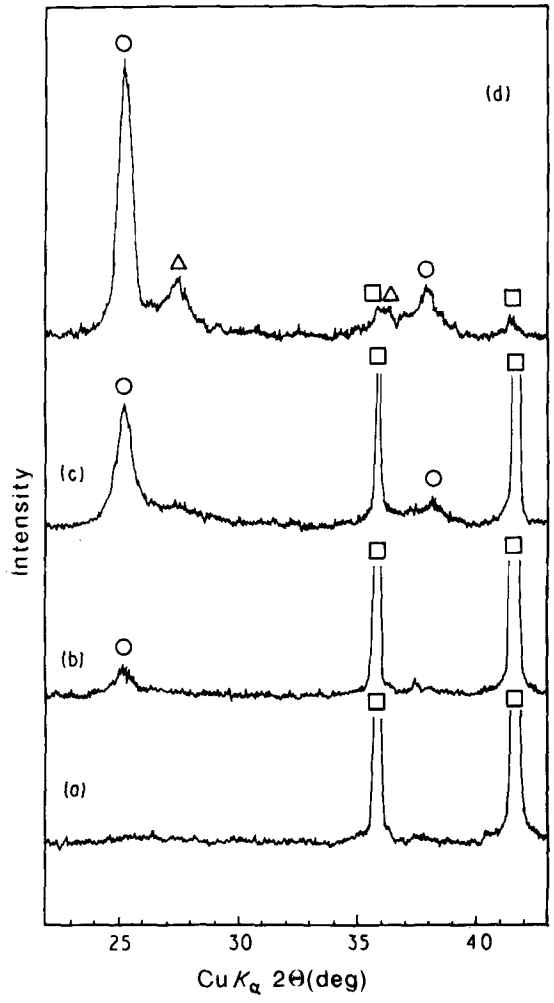

Figure 5 X-ray diffraction patterns of the samples oxidized to various fractions at 400 °C and 3.9 kPa. Reacted fraction (%): (a) 17, (b) 27, (c) 66, (d) 95. (○) Anatase, (△) rutile, (□) TiC.

slight formation of rutile is seen at 400 °C (around 90%), and at 3.9 and 7.9 kPa. At 16 kPa and 400 °C, rutile was formed in amounts comparable to that of

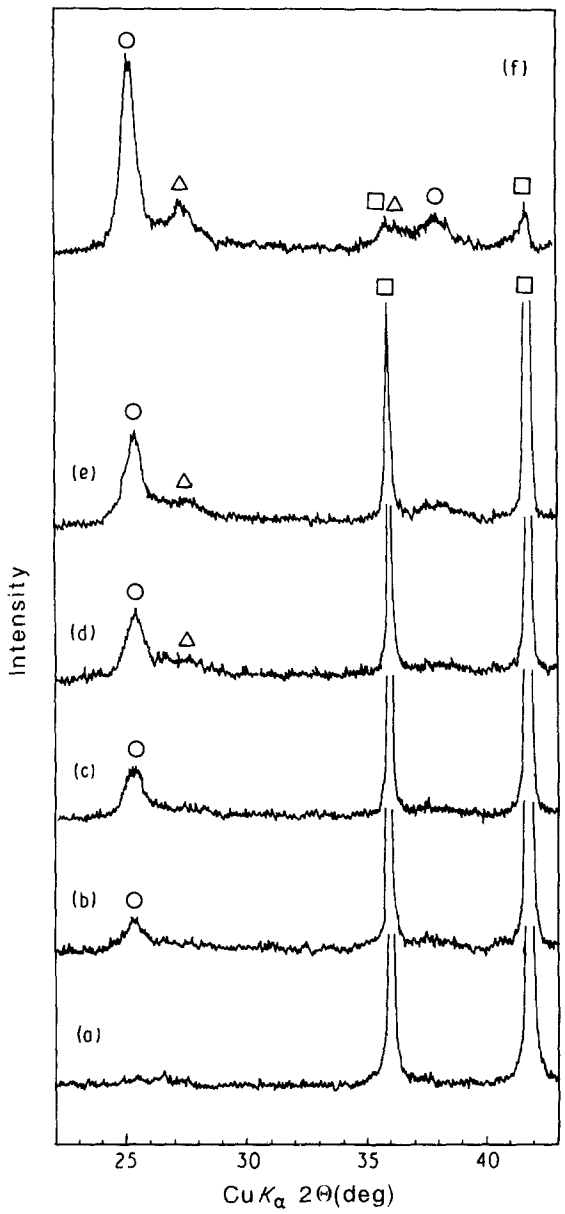

Figure 6 X-ray diffraction patterns of the samples oxidized to various fractions at 400 °C and 7.9 kPa. Reacted fraction (%): (a) 13, (b) 27, (c) 40, (d) 52, (e) 58, (f) 94. (○) Anatase, (△) rutile, (□) TiC.

anatase. The formation of rutile is regarded as resulting from the phase transition from anatase. It is understood that the transition is greatly promoted at 16 kPa (350 and 400 °C) and is enhanced by increasing the temperature from 350 °C to 400 °C (3.9 and 7.9 kPa). It should be emphasized that the transition proceeds at a temperature as low as 350 °C at 7.9 and 16 kPa.

Simultaneous TG–DTA measurement for oxidation of TiC powders was carried out under atmospheric pressure, which corresponds to $P_{O_2} = 20$ kPa (Fig. 9). The DTA curve consists of four exothermic peaks, overlapping each other, below 600 °C, as indicated by the dashed lines. The first broad peak occurs at temperatures of 300–380 °C and below 10%, the second sharp one at 380–410 °C and 10%–20%, the third large one at 410–500 °C and at 20%–58%, and the final broad one above 500 °C and 58%. The fraction ranges of four peaks appearing on the DTA curve correspond roughly to those in steps I–IV.

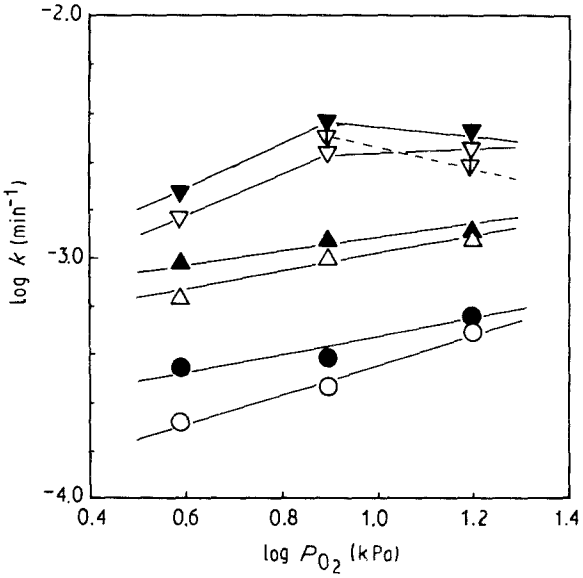

Figure 7 Relationship between log of rate constant and log of oxygen pressure. Reaction temperature (°C): (○, ●) 350, (△, ▲) 376–379, (▽, ▼, ⩛) 400: (▽, △, ○) stage I and II, (▼, ▲, ●) stage III, (⩛) stage IV.

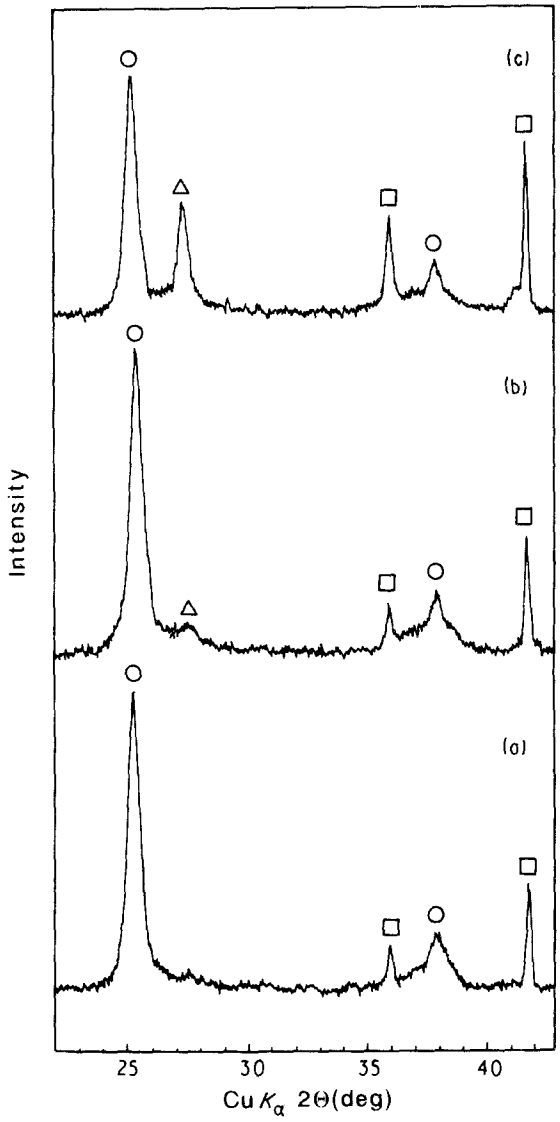

Figure 8 X-ray diffraction patterns of the samples oxidized at 3.9–16 kPa and at 350 °C. Oxygen pressure (kPa): (a) 3.9, (b) 7.9, (c) 16. (○) Anatase; (△) rutile; (□) TiC.

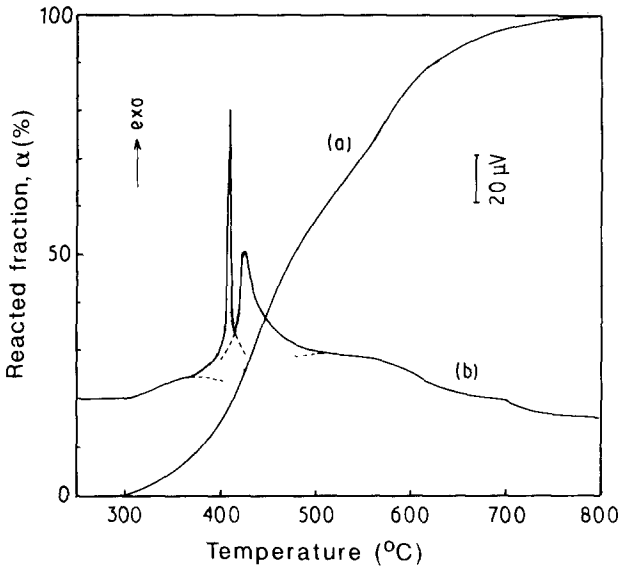

Figure 9 Simultaneous TG–DTA experiment for TiC powders. (a) TG, (b) DTA. Heating rate 5 °C min^{-1} in air, sample weight 18 mg.

SEM observation of the samples oxidized to various fractions was carried out to examine the generation of cracks (Fig. 10). No crack was observed for the samples oxidized below the fraction of 10% at the three pressures. On oxidation up to 30% at 3.9% or 40% at 16 kPa, the grains crack along the edges, as shown in Fig. 10a (see arrows). The cracks become greater with the progression of oxidation (Fig. 10b). When the fraction reaches 80%, some of the grains are completely broken into several pieces (Fig. 10c). The grains on fractured faces are seen to be in the form of pillar shapes with a size of about 0.1 μm.

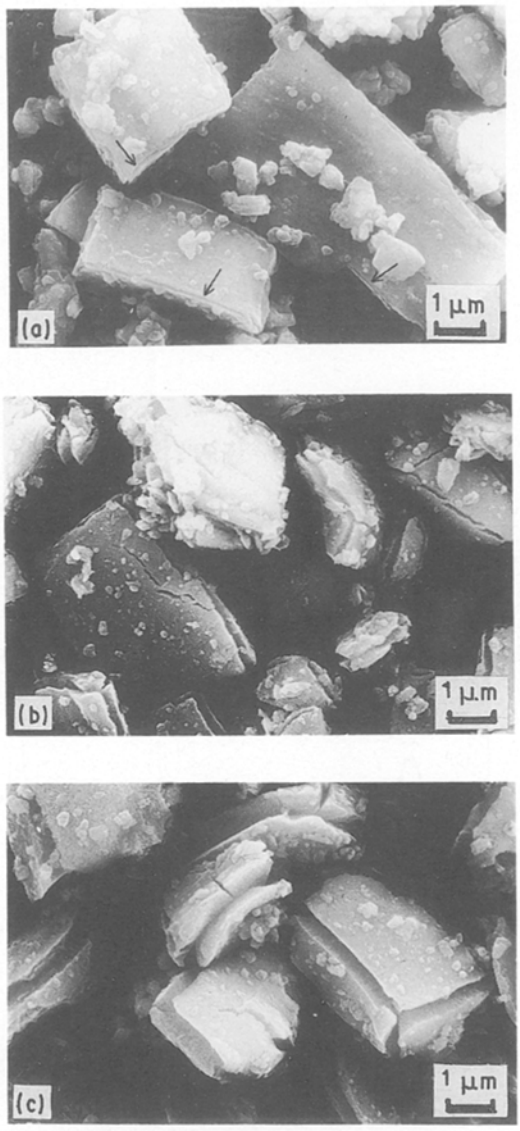

Figure 10 Scanning electron micrographs of the samples oxidized to various fractions. (a) 3.9 kPa, 400 °C, 40%; (b) 3.9 kPa, 400 °C, 53%; (c) 16 kPa, 400 °C, 80%.

4. Discussion

As shown in Fig. 4, the Arrhenius plots change their slopes around 420 °C, giving two activation energies. The observation of two activation energies suggests that the oxidation mechanism must change around this temperature range.

4.1. Oxidation in the low-temperature region

It is recognized that atomic oxygen can be substituted for the carbon present in the interstitial vacancies of the TiC lattice, forming oxycarbide, TiC_xO_{1-x} ($x < 0.5$). The weight increase corresponding to $1 - x = 0.5$ substitution equals 10%. It is believed that oxycarbide forms by dissolution of oxygen into the TiC lattice early in step I: the lattice constant of oxidized TiC powders changed little with increase of the fraction to 20%. X-ray analysis of the samples oxidized below 13%–17% shows the presence of TiC alone (Figs 5 and 6), but the EMD results revealed that the samples oxidized to 6% contain titanium suboxides. Therefore, oxidation in step I involves the formation of oxycarbide/titanium suboxides, and proceeds quickly at 7.9 and 16 kPa, as seen from the intersection of the ordinate at the positive values in the kinetic plots. The fraction by this oxidation at 16 kPa extends to 22%.

The DTA curve shows a very sharp exothermic peak at 18% in step II (Fig. 9). It is seen from XRD (Figs 5 and 6) that anatase is not formed at 13% (3.9 kPa) nor at 17% (7.9 kPa), but is formed at 27%. Referring to this result, a sharp exothermic peak on the DTA curve should be attributed to the crystallization of anatase: an amorphous anatase layer may be formed by oxidation of titanium suboxides early in step II. It is assumed that the double layers consisting of the titanium suboxide and anatase phases are built, acting as a barrier to the diffusion in step II.

The activation energies (125–150 kJ mol^{-1}) in the low-temperature region agree fairly with the energies reported for the oxidation of TiC (205 kJ mol^{-1} [3] and 192 kJ mol^{-1} [5]), and the energies obtained for the parabolic oxidation of titanium metal (109 kJ mol^{-1} [10] and 209 kJ mol^{-1} [11]). It was reported that the energies for oxidation of TiC or titanium are attributable to the diffusion of oxygen through the

oxide layer. Thus, the rate-determining step must be the oxygen diffusion through the titanium suboxide layer in step I, and through the double layers consisting of the titanium suboxide/anatase phase in step II.

In step III, the amount of anatase increases with the progression of oxidation by which the fraction increases to 30%–40% (Figs 5 and 6). With the resulting volume expansion or growth, stress develops within the anatase layer and eventually cracks the grains (Fig. 10a). These cracks provide easy paths for gas transport of oxygen or carbon dioxide, so that the anatase layer no longer acts as a barrier to the diffusion. It should be remembered from the EMD result that at the fraction of 40%, the Ti_2O_3 is present, together with anatase. In step III, only this Ti_2O_3 layer beneath the anatase layer becomes a barrier to the diffusion, so that oxidation in this step is faster than in step II.

As oxidation of the titanium suboxides in step III proceeds, a crack-free anatase layer is again produced. The oxygen must diffuse through the double titanium suboxide/anatase layers. This situation is similar to that in step II. In step IV, a process similar to that in step II should contribute to oxidation. This similarity is supported by the kinetic results that the slopes of α^2–t plots are almost the same as those in step II.

4.2. Oxidation in the high-temperature region

Above 420 °C, oxidation in steps I–III proceeds apparently in one step, up to 45%–50%. High temperatures above 420 °C cause the double titanium suboxide/anatase layers formed in step II to expand more than below that temperature, probably leading to cracking of the layers. Because this cracking continues in step III, oxidation in steps II–III occurs apparently at the same rate. Steward *et al.* [5] have reported that the rates in the oxidation of TiC powders exhibit a maximum at 400–500 °C, and then decrease at 550–600 °C. Lavrenko *et al.* [4] have observed the activation energy around 17 kJ mol^{-1} below 800 °C, which is due to diffusional oxidation of oxycarbide. As understood from these studies, oxidation of TiC proceeds at 400–800 °C in a complex way, no explanation for its mechanism being given.

The above discussion suggests that double titanium suboxide/anatase layers crack in steps II–IV, the oxygen diffusing easily through the layers. The activation energy of 42–71 kJ mol^{-1} obtained might be responsible for the diffusion of oxygen in the oxycarbide phase. The rates in step IV (above 45%–50%) become slower than those in steps I–III. These slower rates may be associated with the formation of rutile in the outermost layer.

5. Conclusion

The isothermal oxidation of TiC powders was performed at temperatures of 350–500 °C at 3.9, 7.9, and 16 kPa. It was found that oxidation proceeds by a diffusion process, consisting of four steps, I (fast step), II (slow step), III (fast step), and IV (slow step). Below about 420 °C, the activation energy was 125–150 kJ mol^{-1}, while it was 42–71 kJ mol^{-1} above that temperature.

In the low-temperature region below about 420 °C, step I involves the formation of the oxycarbide/titanium suboxide layer, and step II the formation of amorphous titanium dioxide by oxidation of the titanium suboxide, accompanied by the crystallization to anatase later in this step. As the crystallization of anatase continues, the resulting volume expansion or growth stress cracks the anatase layer in step III, which provide easy paths for the diffusion. It was demonstrated that the rate-determining step is the oxygen diffusion through the layer of the titanium suboxides in steps II and IV, and through the double layers of titanium suboxide/anatase in step III.

The high-temperatures above 420 °C are sufficient to cause the titanium suboxide and anatase layers to expand more than below that temperature, eventually cracking the layers. As a result, the layers become no barrier to the diffusion of oxygen. The diffusion of oxygen through the oxycarbide phase must be responsible for the low activation energy (42–71 kJ mol^{-1}).

References

1. E. K. STORMS, "The Refractory Carbides" (Academic Press, New York, London, 1967) p. 1.
2. N. F. MACDONALD and C. E. RANSLEY, *Powder Metall.* **3** (1959) 172.
3. M. REICHLE and J. J. NICKL, *J. Less-Common Metals* **27** (1972) 213.
4. Y. A. LAVRENKO, L. A. GLEBOV, A. P. POMITKIN, V. G. CHUPRINA and T. G. PROTSENKO, *Oxid. Metals* **9** (1975) 171.
5. R. W. STEWART and I. B. CUTLER, *J. Amer. Ceram. Soc.* **50** (1967) 176.
6. B. O. HAGLUND and B. LEHTINEN, in "Thermal Analysis", Proceedings of the Third ICTA, Davos (1971) Vol. 3, p. 545.
7. D. K. CHATTERJEE and H. A. LIPSITT, *Metall. Trans.* **13A** (1982) 1837.
8. S. SHIMADA and T. ISHII, *J. Amer. Ceram. Soc.* **73** (1990) 2804.
9. Powder Diffraction File, Cards 23–1078 (TiO), 9–309 (Ti_3O_5), 18–1402 (Ti_4O_7), 10–63 (Ti_2O_3) (Joint Committee on Powder Diffraction Standards, Swarthmore, PA).
10. E. A. GULBRANSEN and K. F. ANDREW, *Met. Trans.* **185** (1949) 744.
11. P. KOFSTAD, P. B. ANDERSON and O. J. KRUDTAA, *J. Less-Common Metals* **3** (1961) 89.

Received 3 December 1990
and accepted 1 May 1991